Biosensors and Bioelectronics 80 (2016) 411–417

Contents lists available at ScienceDirect

Biosensors and Bioelectronics

journal homepage: www.elsevier.com/locate/bios

Detection *EGFR* exon 19 status of lung cancer patients by DNA electrochemical biosensor

Xiong-Wei Xu [a], Xiu-Hua Weng [a,*], Chang-Lian Wang [a], Wei-Wei Lin [a], Ai-Lin Liu [b], Wei Chen [b,*], Xin-Hua Lin [b,*]

[a] Department of Pharmacy, First Affiliated Hospital of Fujian Medical University, Fuzhou, Fujian 350005, PR China
[b] Department of Pharmaceutical Analysis, Fujian Medical University, Fuzhou, Fujian 350004, PR China

ARTICLE INFO

Article history:
Received 12 January 2016
Received in revised form
1 February 2016
Accepted 4 February 2016

Keywords:
Epidermal growth factor receptor
In-frame deletions
Electrochemical biosensor
Non-small cell lung carcinoma
Detection
Lambda exonuclease

ABSTRACT

Epidermal growth factor receptor *(EGFR)* exon 19 mutation status is a very important prediction index for tyrosine kinase inhibitors (TKIs) therapy. In this paper, we constructed a superior selective sandwich-type electrochemical biosensor to detect in-frame deletions in exon 19 of *EGFR* in real samples of patients with non-small cell lung carcinoma. Based on the characteristics of different hybridization efficiency in different hybridization phase conditions, different region around *EGFR* exon 19 deletion hotspots was selected to design DNA probes to improve biosensor performance. The results confirm that alteration of deletion location in target deliberately according to different hybridization phase is able to improve selectivity of sandwich-type DNA biosensor. Satisfactory discrimination ability can be achieved when the deletions are located in the capture probe interaction region. In order to improve efficiency of ssDNA generation from dsDNA, we introduce Lambda exonuclease (λ-exo) to sandwich-type biosensor system. *EGFR* exon 19 statuses of clinical real samples from lung cancer patients can be discriminated successfully by the proposed method. Our research would make the electrochemical biosensor be an excellent candidate for *EGFR* detection for lung cancer patients.

1. Introduction

Lung cancer, the leading cause of cancer death, accounts for about one third of all cancer mortality worldwide due to its high incidence, aggressive tumors behavior, and advanced stage at diagnosis (Shtivelman et al., 2014). Approximately 80% of all lung cancer cases are non-small cell lung carcinoma (NSCLC), which has a poor prognosis with median survival of less than one year when treated by conventional chemotherapy (Schiller et al., 2002). Nowadays, tyrosine kinase inhibitors (TKIs) such as gefitinib and erlotinib are recommended as first-line therapy for selective advanced/metastatic NSCLC because they can remarkably prolong the median survival time. TKIs are preferable for patients whose tumors harbor activating epidermal growth factor receptor (*EGFR*) mutations. *EGFR* is a member of the ErbB receptor tyrosine kinase family. Activation of *EGFR* results in the initiation of a diverse range of cellular signaling pathways, including cell proliferation and protection from apoptosis (Paez et al., 2004; Pao et al., 2004). Activating mutations in the tyrosine kinase domain of the *EGFR* gene have been confirmed to be associated with a dramatic response to the TKIs (Amann et al., 2005; Han et al., 2005).

Activating mutations located in exons 18 to 21 of the *EGFR* tyrosine kinase domain can be found in 10–40% of NSCLC patients, mostly in adenocarcinomas, with higher frequency observed in Asian patients (Sharma et al., 2007). Finding from different studies represents that 44%–80% of *EGFR* mutations are in exon 19, which comprise six types of hotspots deletions (Yamamoto et al., 2009). The deletions located between strand β3 and helix αC can disrupt the inactive conformation of *EGFR* kinase domain and enhance the effectiveness of TKIs (Bose and Zhang, 2009; Yun et al., 2007; Zhang et al., 2006b). Thus, *EGFR* exon 19 mutation status is a very important prediction index for *EGFR* TKIs therapy.

In order to guide treatment regime, mutation analysis of *EGFR* is mandatory to be routinely performed in all patients with advanced adenocarcinoma NSCLC tumor. It is recommended in the NSCLC guidelines from major oncology organizations, such as the National Comprehensive Cancer Network and the American Society of Clinical Oncology. But, so far, there is no guidance recommending specific testing methods or assay attributes. A variety of molecular biology techniques, such as scorpions amplification refractory mutation system, high-resolution melting analysis, and direct automatic sequencing are presently available for the detection of *EGFR* mutations (Hu et al., 2012; Pao and Chmielecki,

* Corresponding authors.
E-mail addresses: shirly0409@163.com (X.-H. Weng), chenandhu@163.com (W. Chen), xhl1963@sina.com (X.-H. Lin).

http://dx.doi.org/10.1016/j.bios.2016.02.009
0956-5663/

2010; Yam et al., 2012). The mostly used method for *EGFR* mutation detection is direct sequencing. However, its widespread utilizations are confined by high cost, limited sensitivity, and time consuming. Other assays for *EGFR* status detection are often limited by their sensitivity, specificity, reproducibility, accuracy, financial and technical constraints. These obstacles underscore the need for advanced analytical principles, prompting the development of alternative methods that are more cost-effective, faster, easier to perform, and more sensitive.

In recent years, an impressive number of electrochemical DNA biosensors have been invented and employed to detect specific nucleotide sequences relied on the high specificity of base paring interactions between complementary strands of DNA (Bonanni and Pumera, 2011; Chen et al., 2012; Dubuisson et al., 2011; Gao et al., 2013; Grabowska et al., 2014; Kannan et al., 2011; Lin et al., 2011; Liu et al., 2008; Ren et al., 2013; Wang et al., 2015; Wu et al., 2010; Xia et al., 2010; Zhang et al., 2007, 2006a). The high sensitivity of electrochemical transducers, as well as their compatibility with modern microfabrication and miniaturization technologies, small dimensions, low cost and power requirements, and their independence of sample turbidity, makes such devices excellent candidates for DNA diagnosis. In this work, we employed sandwich-type electrochemical DNA biosensor to detect in-frame deletions in *EGFR* exon 19, aiming to discriminate the wild and 6 types of hotspots deletion. The crucial point is how to increase the selectivity of the detection system. Based on the characteristics of different hybridization efficiency in different hybridization phase condition, we selected different region around *EGFR* exon 19 deletion hotspots to design DNA probes. Satisfactory discrimination ability was found when the deletions were located in the capture probe interaction region.

Most of the recent reports on DNA biosensor have focused mostly on synthetic oligonucleotides, showing that successful hybridization can be achieved with satisfied sensitivity and selectivity. However, only few studies cast focus on the detection of clinical samples (Campos-Ferreira et al., 2013). The key point is how to effectively generate ssDNA from dsDNA in the sample and make it suitable for the biosensing system. Lambda exonuclease (λ-exo), originating from bacteriophage λ, is a highly processive 5′→3′ dsDNA exonuclease that selectively degrades a phosphorylated chain of the duplex to yield mononucleotides and ssDNA. To the best our knowledge, although λ-exo has been used in various molecular and biological techniques, its applicability in electrochemical DNA biosensor has not been studied. In this work, clinical real samples were successfully detected by λ-exo assisted electrochemical DNA biosensor.

2. Material and methods

2.1. Reagents

Bovine serum albumin was obtained from Roche Diagnostics (Mannheim, Germany) and used without further purification. The 3,3′,5,5′-tetramethylbenzidine (TMB) substrate (Neogen K-blue low-activity substrate) was from Neogen (Lansing, MI). Avidin-horseradish peroxidase (HRP) was from Roche Diagnostics. The buffer solutions used in this study were as follows: The DNA immobilization buffer contained 10 mM Tris–HCl, 1 mM ethylenediaminetetraacetic acid, and 1 M NaCl (pH 8.0). The hybridization buffer was a 10 mM phosphate buffer (PB) solution containing 1 M NaCl (pH 7.4). All solutions were prepared with Milli-Q water (18 MΩ cm resistivity) from a Millipore system.

All oligonucleotides were synthesized and purified by TaKaRa Inc. (Dalian, China), and the sequences are as follows:

Pair C (deletion happen close to 3′-end of target, which will hybridize with capture)

Capture probe: 5′-cggagatgttgcttctcttaattcc-3′
Reporter probe: 5′-ttgatagcgacgggaattttaactt-3′
Target:
wild: 5′-aagttaaaattcccgtcgctatcaaggaattaagagaagcaacatctccg-3′
del1: 5′-aagttaaaattcccgtcgctatcaaaacatctccg-3′
del2: 5′-aagttaaaattcccgtcgctatcaagacatctccg-3′
del3: 5′-aagttaaaattcccgtcgctatcaaggaaccaacatctccg-3′
del4:5′-aagttaaaattcccgtcgctatcaaggaaccatctccg-3′
del5: 5′-aagttaaaattcccgtcgctatcaaggaaccg-3′
del6: 5′-aagttaaaattcccgtcgctatcaaggttccg-3′

Pair C/R (deletion happen in the middle of target which will hybridize with both capture and reporter)

Capture probe: 5′-ttggctttcggagatgttgcttctc-3′
Reporter probe: 5′-ttaattccttgatagcgacgggaat-3′
Target:
wild: 5′-attcccgtcgctatcaaggaattaagagaagcaacatctccgaaagccaa-3′
del1: 5′-attcccgtcgctatcaaaacatctccgaaagccaa-3′
del2: 5′-attcccgtcgctatcaagacatctccgaaagccaa-3′
del3: 5′-attcccgtcgctatcaaggaaccaacatctccgaaagccaa-3′
del4: 5′-attcccgtcgctatcaaggaaccatctccgaaagccaa-3′
del5: 5′-attcccgtcgctatcaaggaaccgaaagccaa-3′
del6: 5′-attcccgtcgctatcaaggttccgaaagccaa-3′

Pair R (deletion happen close to 5-end of target, which will hybridize with reporter)

Capture probe: 5′-catcgaggatttccttgttggcttt-3′
Reporter probe: 5′-cggagatgttgcttctcttaattcc-3′
Target:
wild: 5′-ggaattaagagaagcaacatctccgaaagccaacaaggaaatcctcgatg-3′
del1: 5′-aacatctccgaaagccaacaaggaaatcctcgatg-3′
del2: 5′-gacatctccgaaagccaacaaggaaatcctcgatg-3′
del3: 5′-ggaaccaacatctccgaaagccaacaaggaaatcctcgatg-3′
del4: 5′-ggaaccatctccgaaagccaacaaggaaatcctcgatg-3′
del5: 5′-ggaaccgaaagccaacaaggaaatcctcgatg-3′
del6: 5′-ggttccgaaagccaacaaggaaatcctcgatg-3′

2.2. Electrochemical biosensor preparation

An electrochemical analyzer (CHI440C, Chenhua Co., Shanghai, China) was used for the amperometric and current–time curve experiments was connected to a conventional Au disk working electrode (2 mm diameter), a Ag/AgCl reference electrode, and a Pt wire auxiliary electrode. The BSA-based biosensor was fabricated according to a protocol developed previously (Liu et al., 2013). Briefly, the polished electrode was incubated with 0.1% BSA for 15 min at room temperature. A 3 μL volume of 1 μM capture probe DNA solution was drop cast to cover the BSA-modified gold electrode and incubated for 1 h at room temperature. Finally, the sensor was thoroughly rinsed with water and dried under nitrogen.

2.3. DNA hybridization detection

The DNA detection protocol involved a sandwich-type hybridization assay and the capture of the HRP enzyme tag. Different concentrations of the DNA target were mixed with the biotinylated reporter probe (20 nM) in the hybridization buffer. Then the mixture was incubated with capture probe which had been immobilized on electrode surface, for fixed time at different temperature. A 3 μL volume of avidin-HRP (0.5 U/mL) was spread on the electrode surface for 15 min at room temperature. Finally, the sensor was extensively rinsed and subjected to electrochemical measurements. Amperometric detection was performed in TMB

substrate (Neogen K-blue low-activity substrate) at 0 V, and the current was sampled at 100 s. Each experiment was repeated at least three times.

2.4. ssDNA preparation

2 U of λ-exo (New England Biolabs, China) and 1 × λ-exo reaction buffer (67 mM Glycine-KOH, 2.5 mM $MgCl_2$, and 50 μg/ml BSA) was incubated with 10 nM dsDNA in a total of 100 μL reaction volume at 37 °C for 30 min. The enzyme was then heat inactivated at 75 °C for 10 min. To visualize ssDNA after λ-exo treatment, samples were loaded on a 1.5% agarose gel with ethidium bromide (EB). PCR products concentration was determined using an UV–visible spectrophotometer (UV-2450, Shimadzu Co., Shanghai, China). All samples had been 5′ phosphorylated before λ-exo digestion.

Denaturation by high temperature performed as follow: dsDNA was denatured by heating at 100 °C for 5 min in a water bath, and immediately chilled in ice for 5 min to obtain denatured ssDNA.

2.5. PCR amplification of EGFR from real samples

The real samples came from lung cancer patients who accepted neoplasms resection operation. All patients were from the Chest Surgery Department of First Affiliated Hospital of Fujian Medical University (Fujian, China). Genomic DNA was extracted from liquid-nitrogen-frozen tumor tissue of patients by using Trizol as per manufacturer's instructions (Invitrogen) and DNA was quantified by UV–visible spectrophotometry at 260 nm (SpectrumLab 752 s, China). PCR amplification reaction was set up in 50 μL volume consisting of 5.0 μL 10X buffer (10 mM Tris–HCl, 50 mM KCl, and 1.5 mM $MgCl_2$), 0.2 mM dNTPs, 20 pmol of each primer, 1 μg genomic DNA, and 1.5 μL Taq (Takara, Japan). Amplification was performed on a thermal cycler instrument (MyGenie32, Bioneer, Korea). The reaction comprised initial denaturation at 94 °C for 5 min, followed by 35 cycles of denaturation 94 °C for 30 s, annealing at 57 °C for 30 s, and extension at 72 °C for 30 s. Final extension was carried out at 72 °C for 5 min. Aliquots of 5 μL of the PCR products were electrophoresed on 1.5% agarose gels containing ethidium bromide for 1–1.5 h, then were visualized on an ultraviolet transilluminator and photographed. The 100/200-bp DNA ladder (Fermentas) was used as marker. At the same time, the PCR amplification products were detected by electrochemical analyzer.

EGFR exon 19 was amplified using 6 sets of universal primers with 5′-end phosphorylated respectively:

Primer 1 (134 bp)
Forward primer: 5′-gtcgctatcaaggaattaagag-3′
Reverse primer: 5′-acggtggaggtgaggcagatg-3′
Primer 2 (101 bp)
Forward primer: 5′-ggcacggtgtataagggactc-3′
Reverse primer: 5′-ttgttggctttcggagatgttg-3′
Primer 3 (128 bp)
Forward primer: 5′-acggtgtataagggactctgg-3′
Reverse primer: 5′-gatttccttgttggctttcgg-3′
Primer 4 (202 bp)
Forward primer: 5′-cctcttacacccagtggagaagc-3′
Reverse primer: 5′-ccttgttggctttcggagatg-3′
Primer 5 (100 bp)
Forward primer: 5′-acggtgtataagggactctgg-3′
Reverse primer: 5′-gatttccttgttggctttcgg-3′
Primer 6 (69 bp)
Forward primer: 5′-aagttaaaattcccgtcgctatc-3′
Reverse primer: 5′-ggatttccttgttgggctttcg-3′

3. Results and discussion

3.1. Sequence design

The main purpose of our study was to distinguish wild-type from deletion-type *EGFR*. Therefore, selectivity of the biosensor is a crucial issue. Herein, we attempt to make use of the characteristics of different hybridization efficiency in different phase condition to achieve optimum selectivity. The sandwich-type electrochemical biosensor comprises two types of hybridization, heterogeneous hybridization on the biosensor surface and homogeneous hybridization in solution. Capture probe and a part of target hybridized on the electrode surface, whereas the reporter probe and the other part of target hybridized in solution. Both hybridizations on electrode surface and in solution obey two-state rule. The association of a duplex occurs through the formation of initial contacts involving a small number of bases, due to recognition ability among the bases, followed by zippering of the remainder. The hybridization efficiency is influenced by the formation thermodynamics of DNA duplex, which is dominated by states involving either strongly bound duplexes or widely separated strands (SantaLucia and Hicks, 2004). But unlike homogeneous hybridization in solution, heterogeneous hybridization on solid surface is confined by other extra factors, including steric and electrostatic hindrance present in the DNA probes as well as conformational restriction of the surface-tethered strands. Previous studies have confirmed that, for complementary DNA sequence, surface-hybridization is more difficult than hybridization in solution-phase (Gao et al., 2006). For identical complementary sequences, surface hybridization rates are 20- to 40-fold slower than solution-phase rates. Solution-phase hybridizations are able to achieve 100% hybridization efficiency or completion given equal molar quantities of probe and target, while surface hybridizations reach only 15–25% efficiency under conditions of target saturation (Gao et al., 2006). But for non fully-complementary sequences, whether deletion occurred in different hybridization medium achieve different hybridization efficiency and how did the location of deletion in target influence the selectivity of hybridization remain unknown.

In order to answer these questions and achieve maximum selectivity, we designed 3 sets of DNA sequence as pair C, pair R, and pair C/R (Scheme 1). In pair C, deletion region happened close to 3′-end of target, which will hybridize with capture. In pair R, the deletion region happened close to 5′-end of target, which will hybridize with reporter. In pair C/R, deletion region happened in

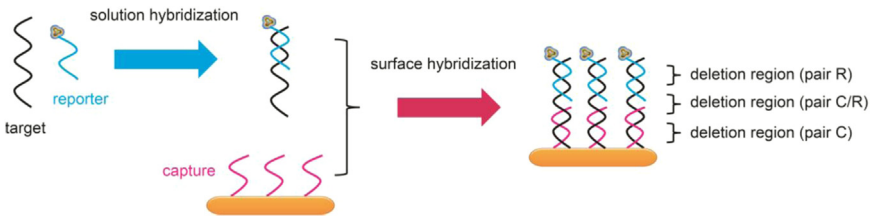

Scheme 1. Schematic illustration of the sequences with different deletion location in target and DNA hybridization in different phase conditions in sandwich-type electrochemical DNA biosensor.

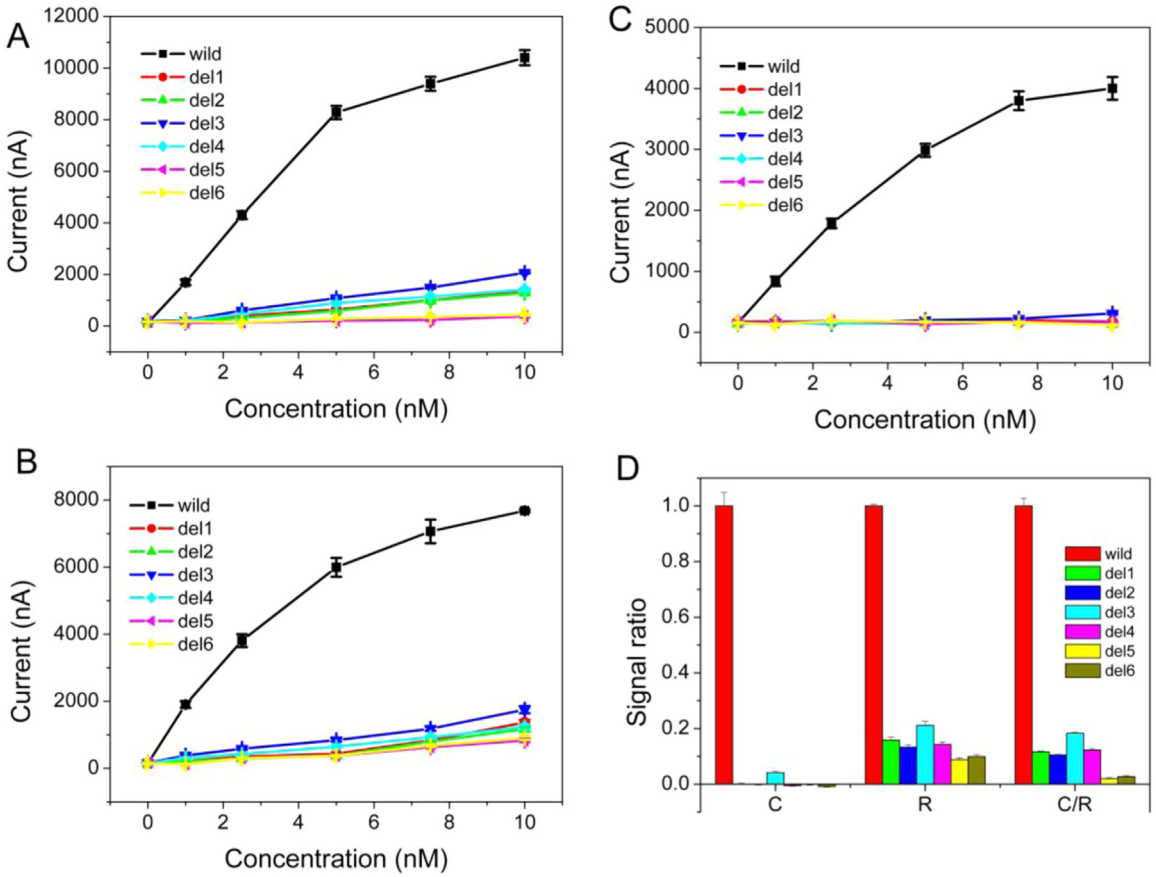

Fig. 1. Amperometric response of wild and 6 types of deletion for (A) pair C/R, (B) pair R, and (C) pair C. (D) The signal ratio of deletions to wild-type target with the same concentration of 10 nM.

the middle of target, which will hybridize with both capture and reporter. Comparative experiments were performed to assess which one responded more selectively to wild-type sequence than 6 types of hotspot deletion *EGFR* including 10-base deletion (del3), 12-base deletion (del4), 15-base deletion (del1 and del2), and 18-base deletion (del5 and del6). As shown in Fig. 1A–C, 3 sets of DNA sequence exhibited different performance. Since the wild-type sequences were fully complementary to capture and reporter, they showed higher amperometric responses than deletion-type sequences. Signal of 6 types of deletion *EGFR* augmented along with the decrease of deletion base numbers. Del3 showed the highest signal among 6 deletion types, followed by del1, del2, del4, del5, and del6 for pair C/R and pair R. But for pair C, in addition to get lowest del3 signal among 3 sets of DNA, signals of other 5 deletion-types showed almost no different form that of blank. As showed in Fig. 1D, the signal ratio of 10 nM del3 to wild-type target with the same concentration is about 21.1% for pair R, 18.3% for pair C/R, whereas only 4.1% for pair C. These results confirmed that the location of deletion in target play an important role in sandwich-type biosensor. Furthermore, the presence of non-complementary DNA sequence such as mismatch or deletion would have more negative impact on surface-hybridization than that in solution. By making use of the characteristics that hybridization efficiency varied in different phase and consequently altering deletion location deliberately, well discrimination between wild and deletions can be achieved. To best distinguish wild-type from deletion-type *EGFR*, pair C was used in the following studies and real sample detection.

3.2. *ssDNA production from dsDNA*

The sandwich-type DNA biosensor is suitable for ssDNA detection, but DNA in real samples is double-stranded. Various methods such as asymmetric PCR, biotin-streptavidin separation, size separation on denaturing urea polyacrylamide gel electrophoresis, and high-temperature denaturalization have been used for preparation ssDNA (Marimuthu et al., 2012). However, these methods exhibit different disadvantages. Asymmetric PCR is the most economical approach of generating ssDNA from dsDNA template. However, subsequent purification of ssDNA is needed since both ssDNA and dsDNA generates in asymmetric PCR. In addition, it is difficult to optimum the ratio of primer amounts for asymmetric PCR. Biotin-streptavidin separation may affect sandwich-type biosensor by taking biotin-streptavidin into the system. Size separation on denaturing urea polyacrylamide gel electrophoresis is tedious and time-consuming. Many investigations used high-temperature denaturalization to generate ssDNA for biosensing due to it is economic, convenient and easy to perform (Chen et al., 2008; Rai et al., 2012a, 2012b). But the inherent and fatal weakness of this approach is that renaturation in the solution is rather predominant than hybridization on the sensor surface.

In order to improve efficiency of ssDNA generation from dsDNA, we attempted to introduce λ-exo to sandwich-type biosensor system. The λ-exo-assisted production of ssDNA has been applied in technologies such as next-generation sequencing platforms (Ball et al., 2009), DNA-chips (Brinker et al., 2010), SELEX (Avci-Adali et al., 2010), subtractive hybridization techniques (Low et al., 2001), and sample preparation for electrospray ionization

mass spectrometry (Null et al., 2000). However, whether λ-exo could be employed in sandwich-type biosensor without unfavorable impact remains unknown. In this study, λ-exo digestion couple with sandwich-type DNA biosensing system was investigated and compared to high-temperature denaturation.

As shown in Fig. 2, current signal of dsDNA group was the same as blank, revealing that no hybridization event happened on the electrode surface. After high-temperature denaturation, a positive response was obtained. However, pretreatment by high-temperature denaturation is hard to get efficient and satisfied ssDNA generation because that renaturation will happen quickly once conditions permit. The current of high-temperature denaturation group was only 21.6% of that obtained in the presence of ssDNA target. On the contrary, dsDNA pretreated by λ-exo digestion achieved efficient hybridization on the electrode surface. λ-exo can selectively degrade the phosphorylated chain of dsDNA, and remains the complementary chain and mononucleotides. Unlike high temperature denaturation, renaturation will not happen in any condition after λ-exo digestion, which is beneficial for DNA to keep in single-stranded status, consequently ensure the hybridization event successfully happened in the biosensing system. Most importantly of all, the current signal obtained from λ-exo digestion group was the same as that of synthesized ssDNA. This revealed that λ-exo and the treatment procedure have no extra impact on the sandwich-type biosensor. Therefore, λ-exo pretreatment procedure can be great potential for real sample applications.

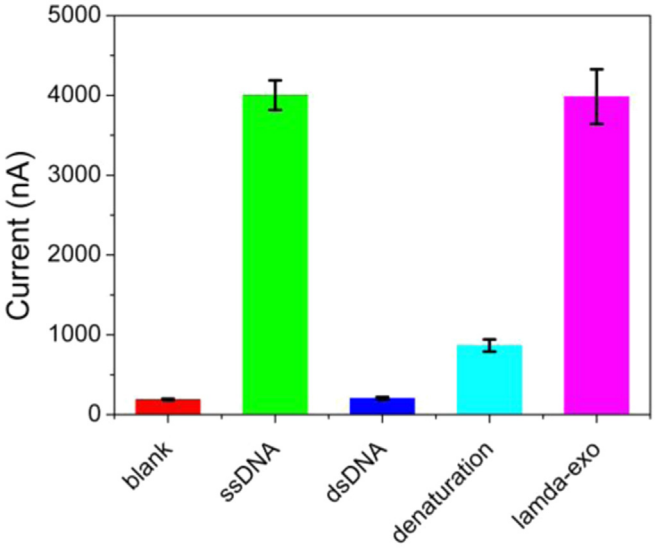

Fig. 2. Amperometric response of dsDNA before and after pretreatment by high-temperature denaturation and λ-exo digestion.

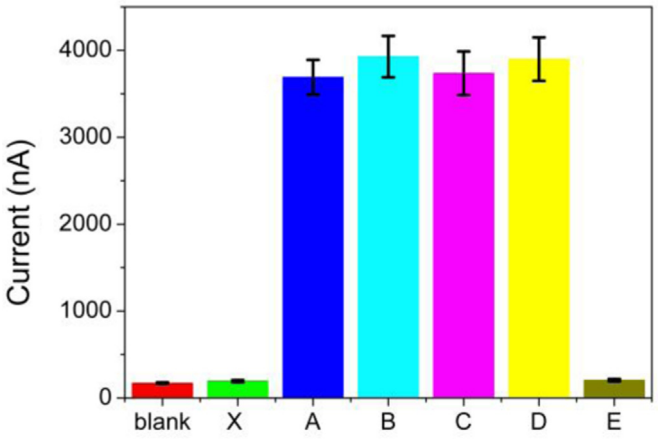

Fig. 4. Amperometric response of the biosensor to PCR products of real sample. X, PCR product of patient A without λ-exo digestion. A to E, PCR products of patient A to E after λ-exo digestion.

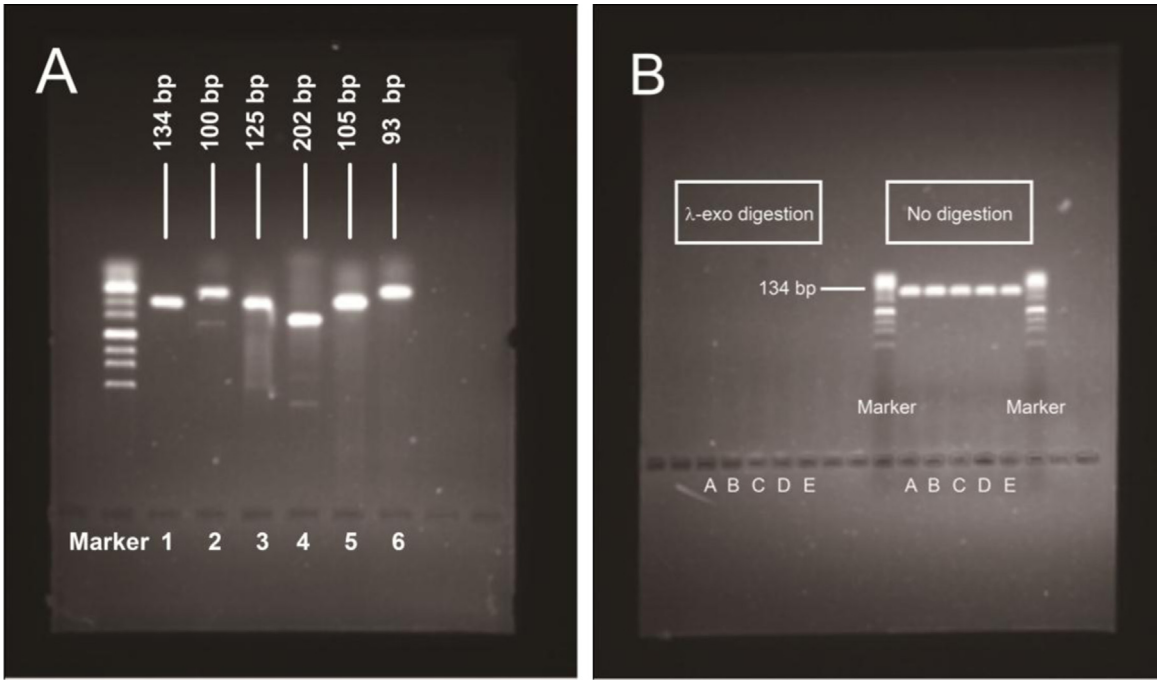

Fig. 3. (A) Analysis of the PCR amplicon in 1.5% agarose gel electrophoresis containing 0.5 μg/mL ethidium bromide. lane 1–6: universal primer 1–6 for patient A. (B) Gel electrophoresis for PCR products with or without λ-exo digestion. Left: PCR products of patient A–E after λ-exo digestion. Right: PCR products of patient A–E without λ-exo digestion.

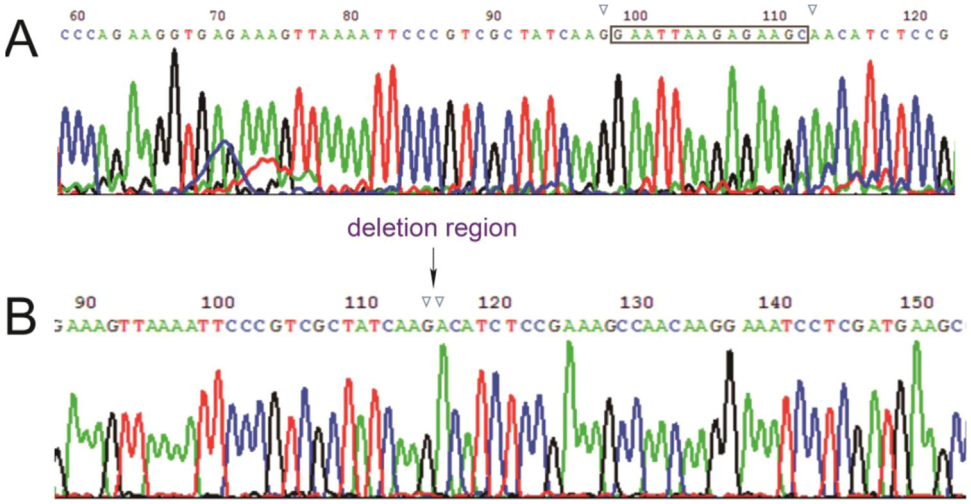

Fig. 5. Gene sequencing graph of the *EGFR* gene PCR amplification product. (A) Wild *EGFR* (patient A–D). (B) Deletion in *EGFR* exon 19 (patient E).

3.3. Detection EGFR exon 19 status of lung cancer patients

Tumor tissues were came from five lung cancer patients (A to E) who underwent resection. DNA genomes were extracted from tumor tissues, followed by PCR amplification. Due to the uncertainties of gene type of real samples, we designed six kinds of universal primers (primer 1–6) to make sure target sequence amplified successfully no matter the sample was wild or deletion type *EGFR*. As shown in Fig. 3A, PCR products of sample A using different primers were visualized by gel electrophoresis. Among six kinds of universal primers, primer 1 (134 bp) exhibited more excellent performance than others with higher light band and less tailing. We therefore chose primer 1 as optimal condition for further investigation.

Gel electrophoresis was further performed to confirm the successful generation of ssDNA by λ-exo digestion. Double-stranded and single-stranded DNA can be distinguished visually by EB staining. EB strongly binds to dsDNA molecules to produce light bands whereas no visualization for ssDNA due to weaker binding of EB to ssDNA. As shown in Fig. 3B, the λ-exo digestion products did not present any light bands in 1.5% agarose gel, revealing the success of ssDNA generation.

The PCR products were diluted to 10 nM and pretreated by λ-exo digestion. The ssDNA sequences were then assayed by sandwich-type electrochemical biosensor. Unlike synthetic ssDNA detection, there were extra handlings for real samples, including PCR amplification and λ-exo digestion. These procedures might yield some constituents to real sample detection system. The influence of λ-exo digestion to detection system has already been excluded in previous section. We therefore detected PCR products without λ-exo digestion to elucidate whether those constituents from PCR procedure, such as primers, DNA template, DNA polymerase, and dNTP would cast impact on real sample detection system. As shown in Fig. 4, the current signal of PCR product without λ-exo digestion was similar to blank. This result demonstrates that the constituents from PCR procedure had no obvious influence on biosensing system, neither hindered hybridization nor developed false positive signal.

The current responses of real samples A to D were approximately 3500-4000 nA, which were consistent with that of synthetic wild-type *EGFR* ssDNA. Sequencing result further confirmed the wild genotype of patients A to D (Fig. 5A). As for patient E, the obtained current was only 295 nA, corresponding to deletion *EGFR* genotype. Sequencing result shows that the del2 genotype happened in patient E (Fig. 5B). All the results obtained from the proposed biosensor were completely concordant with those of sequencing analysis, indicating the success of real sample detection and discrimination between wild and deletions in exon 19 of *EGFR*.

The proposed biosensor overcomes some disadvantages of traditional sequencing assay attributing to its time-saving, low-cost, high selectivity as well as simple and convenient operation. The assay could be finished within 3.5 h, which is beneficial for patients to select therapy regimens as soon as possible. And low cost of biosensor detection would make more and more patients afford detection cost and finally propel *EGFR* detection to be performed regularly and prevalently.

4. Conclusions

In this work, DNA electrochemical biosensor was designed to detection *EGFR* exon 19 statuses of lung cancer patients. The strategy that alters deletion location in target deliberately according to different hybridization phase is able to improve selectivity of sandwich-type DNA biosensor. These findings may have implications for the design of biosensors with better performance. Meanwhile, we attempt to employ λ-exo to digest PCR products of clinical real samples to generate ssDNA target. The experimental results show that λ-exo can be employed for the sandwich-type biosensing system without any negative influence. Combined these two strategies, we can detect PCR amplified real samples with satisfied results and discriminate deletion-type from wild-type *EGFR* with high selectivity. Compared with traditional methods, the proposed biosensor detection method exhibits advantages such as time-saving, economic, high selectivity, which will urge this assay to be a promising method for the potential use in medical diagnosis for lung cancer patients. Furthermore, these strategies are expected to have further extensive applications in other DNA detection.

Acknowledgment

The authors gratefully acknowledge the financial support of the National High Technology and Development of China (863 Project, 2012AA022604), the National Natural Science Foundation of China (21275028), Research Fund for the Doctoral Program of Higher Education of China (20123518110001), the Natural Science Foundation of Fujian Province (2015J01415), the Medical Elite Cultivation Program of Fujian (2013-ZQN-ZD-21, 2013-ZQN-JC-23).

References

Amann, J., Kalyankrishna, S., Massion, P.P., Ohm, J.E., Girard, L., Shigematsu, H., Peyton, N., Juroske, D., Huang, Y., Salmon, J.S., Kim, Y.H., Pollack, J.R., Yanagisawa, K., Gazdar, A., Minna, J.D., Kurie, J.M., Carbone, D.P., 2005. Cancer Res. 65, 226–235.

Avci-Adali, M., Paul, A., Wilhelm, N., Ziemer, G., Wendel, H.P., 2010. Molecules 15, 1–11.

Ball, M.P., Li, J.B., Gao, Y., Lee, J.H., LeProust, E.M., Park, I.H., Xie, B., Daley, G.Q., Church, G.M., 2009. Nat. Biotechnol. 27, 361–368.

Bonanni, A., Pumera, M., 2011. ACS Nano 5, 2356–2361.

Bose, R., Zhang, X.W., 2009. Exp. Cell Res. 315, 649–658.

Brinker, A., Schulze, H., Bachmann, T., Moller, R., 2010. Biosens. Bioelectron. 26, 898–902.

Campos-Ferreira, D.S., Nascimento, G.A., Souza, E.V.M., Souto-Maior, M.A., Arruda, M.S., Zanforlin, D.M.L., Ekert, M.H.F., Bruneska, D., Lima, J.L., 2013. Anal. Chim. Acta 804, 258–263.

Chen, J.H., Zhang, J., Wang, K., Lin, X.H., Huang, L.Y., Chen, G.N., 2008. Anal. Chem. 80, 8028–8034.

Chen, W., Liu, Y.-H., Li, H.-N., Liu, A.-L., Lin, X.-H., Chen, Y.-Z., 2012. Anal. Chim. Acta 748, 89–94.

Dubuisson, E., Yang, Z.Y., Loh, K.P., 2011. Anal. Chem. 83, 2452–2460.

Gao, H., Jiang, X., Dong, Y.J., Tang, W.X., Hou, C., Zhu, N.N., 2013. Biosens. Bioelectron. 48, 210–215.

Gao, Y., Wolf, L.K., Georgiadis, R.M., 2006. Nucleic Acids Res. 34, 3370–3377.

Grabowska, I., Singleton, D.G., Stachyra, A., Gora-Sochacka, A., Sirko, A., Zagorski-Ostoja, W., Radecka, H., Stulz, E., Radecki, J., 2014. Chem. Commun. 50, 4196–4199.

Han, S.W., Kim, T.Y., Hwang, P.G., Jeong, S., Kim, J., Choi, I.S., Oh, D.Y., Kim, L.H., Kim, D.W., Chung, D.H., Im, S.A., Kim, Y.T., Lee, J.S., Heo, D.S., Bang, Y.J., Kim, N.K., 2005. J. Clin. Oncol. 23, 2493–2501.

Hu, C.J., Liu, X.L., Chen, Y.J., Sun, X.M., Gong, Y.W., Geng, M., Bi, L.Q., 2012. Oncol. Rep. 28, 1815–1821.

Kannan, B., Williams, D.E., Booth, M.A., Travas-Sejdic, J., 2011. Anal. Chem. 83, 3415–3421.

Lin, L.Q., Liu, Q.C., Wang, L.M., Liu, A.L., Weng, S.H., Lei, Y., Chen, W., Lin, X.H., Chen, Y.Z., 2011. Biosens. Bioelectron. 28, 277–283.

Liu, G., Wan, Y., Gau, V., Zhang, J., Wang, L.H., Song, S.P., Fan, C.H., 2008. J. Am. Chem. Soc. 130, 6820–6825.

Liu, Y.H., Li, H.N., Chen, W., Liu, A.L., Lin, X.H., Chen, Y.Z., 2013. Anal. Chem. 85, 273–277.

Low, R.K.W., Prakash, A.P., Swarup, S., Goh, C.J., Kumar, P.P., 2001. Anal. Biochem. 295, 240–247.

Marimuthu, C., Tang, T.H., Tominaga, J., Tan, S.C., Gopinath, S.C.B., 2012. Analyst 137, 1307–1315.

Null, A.P., Hannis, J.C., Muddiman, D.C., 2000. Analyst 125, 619–625.

Paez, J.G., Janne, P.A., Lee, J.C., Tracy, S., Greulich, H., Gabriel, S., Herman, P., Kaye, F.J., Lindeman, N., Boggon, T.J., Naoki, K., Sasaki, H., Fujii, Y., Eck, M.J., Sellers, W.R., Johnson, B.E., Meyerson, M., 2004. Science 304, 1497–1500.

Pao, W., Chmielecki, J., 2010. Nat. Rev. Cancer 10, 760–774.

Pao, W., Miller, V., Zakowski, M., Doherty, J., Politi, K., Sarkaria, I., Singh, B., Heelan, R., Rusch, V., Fulton, L., Mardis, E., Kupfer, D., Wilson, R., Kris, M., Varmus, H., 2004. Proc. Natl. Acad. Sci. USA 101, 13306–13311.

Rai, V., Deng, J.J., Toh, C.S., 2012a. Talanta 98, 112–117.

Rai, V., Hapuarachchi, H.C., Ng, L.C., Soh, S.H., Leo, Y.S., Toh, C.S., 2012b. Plos One, 7.

Ren, Y.Q., Deng, H.M., Shen, W., Gao, Z.Q., 2013. Anal. Chem. 85, 4784–4789.

SantaLucia, J., Hicks, D., 2004. Annu. Rev. Biophys. Biomol. Struct. 33, 415–440.

Schiller, J.H., Harrington, D., Belani, C.P., Langer, C., Sandler, A., Krook, J., Zhu, J.M., Johnson, D.H., Eastern Cooperative Oncology Group, 2002. N. Engl. J. Med. 346, 92–98.

Sharma, S.V., Bell, D.W., Settleman, J., Haber, D.A., 2007. Nat. Rev. Cancer 7, 169–181.

Shtivelman, E., Hensing, T., Simon, G.R., Dennis, P.A., Otterson, G.A., Bueno, R., Salgia, R., 2014. Oncotarget 5, 1392–1433.

Wang, K., Lei, Y., Zhong, G.X., Zheng, Y.J., Sun, Z.L., Peng, H.P., Chen, W., Liu, A.L., Chen, Y.Z., Lin, X.H., 2015. Biosens. Bioelectron. 71, 463–469.

Wu, J., Campuzano, S., Halford, C., Haake, D.A., Wang, J., 2010. Anal. Chem. 82, 8830–8837.

Xia, F., White, R.J., Zuo, X., Patterson, A., Xiao, Y., Kang, D., Gong, X., Plaxco, K.W., Heeger, A.J., 2010. J. Am. Chem. Soc. 132, 14346–14348.

Yam, I., Lam, D.C.L., Chan, K.M., Ho, J.C.M., Ip, M., Lam, W.K., Chan, T.K., Chan, V.V., 2012. J. Thorac. Oncol. 7, 1131–1140.

Yamamoto, H., Toyooka, S., Mitsudomi, T., 2009. Lung Cancer 63, 315–321.

Yun, C.H., Boggon, T.J., Li, Y.Q., Woo, M.S., Greulich, H., Meyerson, M., Eck, M.J., 2007. Cancer Cell 11, 217–227.

Zhang, J., Song, S., Wang, L., Pan, D., Fan, C., 2007. Nat. Protoc. 2, 2888–2895.

Zhang, J., Song, S.P., Zhang, L.Y., Wang, L.H., Wu, H.P., Pan, D., Fan, C.H., 2006a. J. Am. Chem. Soc. 128, 8575–8580.

Zhang, X.W., Gureasko, J., Shen, K., Cole, P.A., Kuriyan, J., 2006b. Cell 125, 1137–1149.